Conformational and Thermodynamic Characterization of the Molten Globule State Occurring during Unfolding of Cytochromes-c by Weak Salt Denaturants†

Shabir H. Qureshi,‡ Beenu Moza,‡ Sushma Yadav,§ and Faizan Ahmad*

Department of Biosciences, Jamia Millia Islamia, Jamia Nagar, New Delhi - 110 025, India

Received November 1, 2002; Revised Manuscript Received December 20, 2002

ABSTRACT: The denaturation of bovine and horse cytochromes-c by weak salt denaturants (LiCl and $CaCl_2$) was measured at 25 °C by observing changes in molar absorbance at 400 nm ($\Delta\epsilon_{400}$) and circular dichroism (CD) at 222 and 409 nm. Measurements of $\Delta\epsilon_{400}$ and mean residue ellipticity at 409 nm ($[\theta]_{409}$) gave a biphasic transition for both modes of denaturation of cytochromes-c. It has been observed that the first denaturation phase, N (native) conformation ↔ X (intermediate) conformation and the second denaturation phase, X conformation ↔ D (denatured) conformation are reversible. Conformational characterization of the X state by the far-UV CD, 8-anilino-1-naphthalene sulfonic acid (ANS) binding, and intrinsic viscosity measurements led us to conclude that the X state is a molten globule state. Analysis of denaturation transition curves for the stability of different states in terms of Gibbs energy change at pH 6.0 and 25 °C led us to conclude that the N state is more stable than the X state by 9.55 ± 0.32 kcal mol^{-1}, whereas the X state is more stable than the D state by only 1.40 ± 0.25 kcal mol^{-1}. We have also studied the effect of temperature on the equilibria, N conformation ↔ X conformation and X conformation ↔ D conformation in the presence of different denaturant concentrations using two different optical probes, namely, $[\theta]_{222}$ and $\Delta\epsilon_{400}$. These measurements yielded T_m, (midpoint of denaturation) and ΔH_m (enthalpy change) at T_m as a function of denaturant concentration. A plot of ΔH_m versus corresponding T_m was used to determine the constant-pressure heat capacity change, ΔC_p ($= (\partial\Delta H_m/\partial T_m)_p$). Values of ΔC_p for N conformation ↔ X conformation and X conformation ↔ D conformation is 0.92 ± 0.02 kcal mol^{-1} K^{-1} and 0.41 ± 0.01 kcal mol^{-1} K^{-1}, respectively. These measurements suggested that about 30% of the hydrophobic groups in the molten globule state are not accessible to the water.

The pathway by which a newly synthesized polypeptide chain spontaneously folds to its native functional form is still a central goal of the protein chemists. In recent years, great interest has been focused on detecting and characterizing the intermediates that might be formed during the folding of proteins. The "molten globule" (MG) is one such intermediate of significance. It is being intensively studied by both kinetic and equilibrium methods because of its possible implication in the folding process of several proteins. Equilibrium molten globules are important tools to study protein folding because they are much easier to structurally characterize than kinetic intermediates. The common structural characteristics of molten globule state are (*1*) as follows: (i) the presence of pronounced amount of secondary structure, (ii) the absence of most of the specific tertiary structure produced by the tight packing of side chains, (iii) the compactness of the protein molecule with the radius of gyration 10−30% larger than the native (N) state, (iv) the presence of a loosely packed hydrophobic core that increases the hydrophobic surface accessible to solvent. The molten globule state of proteins is often observed under mildly denaturing conditions, e.g., moderate concentrations of strong denaturants such as guanidine hydrochloride and urea (*2*, *3*), at acidic or alkaline pH with or without stabilizing ions (*4*−*6*), and heat (*7*). To date, most of the studies on molten globule state of cytochrome-c are in extreme conditions only, i.e., in acidic solution at pH 2 containing high salt concentration or when positive charges at acidic pH are neutralized by anions (*4*, *8*, *9*).

While the formation of molten globule from the acid denatured horse cytochrome-c in the presence of salt at pH 2.0 has been widely studied, little progress has been made to detect an on pathway MG during folding ↔ unfolding induced by denaturants near neutral pH. However, occurrence of MG state has been speculated during the denaturation of cytochrome-c by urea and guanidine hydrochloride (*10*−*12*). We have been interested for some time in the conformational and thermodynamic characterization of denaturation of proteins by weak salt denaturants such as LiCl and $CaCl_2$ (*13*−*19*). These weak salt denaturants have been shown to induce a biphasic denaturation curve monitored by absorption of horse ferricytochrome-c in the Soret band region (*17*, *18*). We report here the results on the structural and thermodynamic characterization of the intermediate state occurring on the pathway between the native and denatured states of

† Supported by the Council of Scientific and Industrial Research (India) Grant (37/(976)/98-EMR), and Department of Science and Technology (India) Grant (SP/SOD/26/96).

* Corresponding author. E mail: faizana@del3.vsnl.net.in. Fax: 91-11-2698-1232.

‡ These authors contributed equally to this work.

§ Present address: Department of Chemistry and Biochemistry, University of Texas at Arlington, Arlington, Texas 76019.

10.1021/bi0271042 CCC: $25.00
Published on Web 01/24/2003

horse and bovine cytochromes-c using measurements of (i) the far-UV circular dichroism (an index of secondary structure), (ii) near-UV circular dichroism (an index of packing of side chains), (iii) intrinsic viscosity (a measure of radius of gyration), and (iv) 8-anilino-1-naphthalene sulfonic acid (ANS)[1]−protein interaction (a measure of presence of hydrophobic clusters accessible to the solvent). These measurements led us to conclude that the intermediate state of both the proteins has all the common structural characteristics of MG (*1*).

Thermodynamic stability parameters associated with the unfolding transition are important in the understanding of physical mechanism of MG formation and its relation to protein folding. Thermodynamic stability parameters associated with the transition between MG and acid denatured states of horse cytochrome-c have been measured (*7*, *9*, *48*). However, there is no report on the measurements of these parameters associated with formation of MG from the native protein. In this study, we have measured all the thermodynamic parameters to describe transition between the N and MG states and between the MG and denatured states, and report that native structure of horse and bovine cytochromes-c is stabilized mainly by hydrophobic interactions, and secondary structure contributes little to the protein stability.

MATERIALS AND METHODS

Commercial lyophilized chromatographically purified horse heart cytochrome-c (type IV) and bovine heart cytochrome-c were purchased from Sigma Chemical Company. Since both proteins gave a single band on SDS−PAGE, they were used without further purification. Lithium chloride, sodium salt of cacodylic acid, and ANS were from Sigma Chemical Company. Calcium chloride and potassium chloride were from Merck (India). These and other chemicals were analytical-grade reagents.

Horse and bovine cytochromes-c samples were oxidized first by adding 0.1% potassium ferricyanide as described earlier (*5*). The concentration of the oxidized horse cytochrome-c (h-cyt-c) and that of bovine cytochrome-c (b-cyt-c) were determined experimentally using a value of 106 000 M^{-1} cm^{-1}, the molar absorption coefficient (ϵ) at 409 nm (*20*). Concentration of stock solutions of LiCl and $CaCl_2$ were determined by measuring the difference refractive index of each solution and 0.03 M cacodylate buffer containing 0.1 M KCl (*21*). Concentration of the stock solution of ANS was determined spectrophotometrically using a value of 5000 M^{-1} cm^{-1} for ϵ at 350 nm (*22*). For optical measurements all solutions were prepared in the 0.03 M cacodylate buffer containing 0.1 M KCl at pH 6.0 and equilibrated overnight at room temperature.

The absorption measurements of each protein were carried out in a Shimadzu-2100 UV−Vis spectrophotometer and a Jasco V-560 UV/VIS spectrophotometer whose temperature was regulated by circulating water from an external thermostated water bath and by a peltier-type temperature controller (ETC-505T), respectively. Isothermal denaturation curves of both cyt-c preparations induced by weak salt denaturants (LiCl and $CaCl_2$) at 25.0 ± 0.1 °C was measured in Shimadzu spectrophotometer. Protein concentrations for the spectral measurements were 7−10 μM in the Soret region. The thermal denaturation of proteins in the presence and absence of different concentrations of both denaturants were carried out in Jasco UV/Vis spectrophotometer with a heating rate of 1 °C/min. The change in the absorbance at 400 nm of proteins was measured in the temperature range 20−85 °C. These isothermal and thermal denaturations of h-cyt-c and b-cyt-c were also measured in a Jasco spectropolarimeter (model J-715) equipped with a peltier-type temperature controller (PTC-348 WI). Protein concentration used for CD measurements was in the range 18−20 μM, and 0.1 and 1.0 cm cells were used for the far-UV and Soret region measurements, respectively. CD instrument was routinely calibrated with D-10-camphorsulfonic acid. The results of all the CD measurements are expressed as mean residue ellipticity ($[\theta]_\lambda$) in deg cm^2 $dmol^{-1}$ at a given wavelength λ (nm) using the relation

$$[\theta]_\lambda = \theta_\lambda M_o/10cl \qquad (1)$$

where θ_λ is the observed ellipticity in millidegrees at wavelength λ, M_o is the mean residue weight of the protein, c is the protein concentration (mg/cm^3), and l is the path length (cm). It should be noted that each observed θ_λ of the protein was corrected for the contribution of the solvent.

Fluorescence spectra were measured in a Perkin-Elmer L-50 spectroluminescencemeter in a 5-mm quartz cell at 25 °C, with both excitation and emission slits set at 12 nm. Protein concentration for all the experiments was in the range 7−10 μM. For the ANS fluorescence in ANS−protein binding experiments, the excitation wavelength was 360 nm and emission spectra were recorded from 400 to 600 nm.

Viscosity measurements were carried out in an Ostwald type viscometer with a flow rate of 60 s for 1 mL of distilled water. Viscometer was kept in a thermostated water bath to maintain the temperature of samples at 25.0 ± 0.1 °C. Protein concentration used was in the range 2.0−25.0 mg mL^{-1}. As described earlier (*23*), the reduced viscosity (η_{red}) of the protein was determined at different protein concentrations using the relation

$$\eta_{red} = (t - t_o)/t_o c + (1 - (\bar{v}_2 \rho_o))/\rho_o \qquad (2)$$

where t_o and t are the times of fall of 1 mL of solvent and 1 mL of protein solution, respectively, c is the protein concentration in g mL^{-1}, $\bar{v}_2$ is the partial specific volume of cyt-c, which is equal to 0.724 mL g^{-1} (*24*), and ρ_o is the density of the solvent.

Reversibility of the isothermal denaturation by LiCl and $CaCl_2$ was checked using the procedure described earlier (*25*). Reversibility of the thermal denaturation was checked by matching the optical property before and after the denaturation.

RESULTS

LiCl- and $CaCl_2$-induced denaturations of ferricytochromes-c from horse and bovine hearts were measured by observing changes in the absorption at 400 nm and circular dichroism (CD) at 222 and 409 nm at pH 6.0 (0.03 M cacodylate buffer containing 0.1 M KCl) and 25 ± 0.1 °C. Each stable state of the denaturation equilibria was character-

[1] Abbreviations: cyt-c, cytochrome-c; CD, circular dichroism; ANS, 8-anilino-1-naphthalene sulfonic acid; DSC, differential scanning calorimetry.

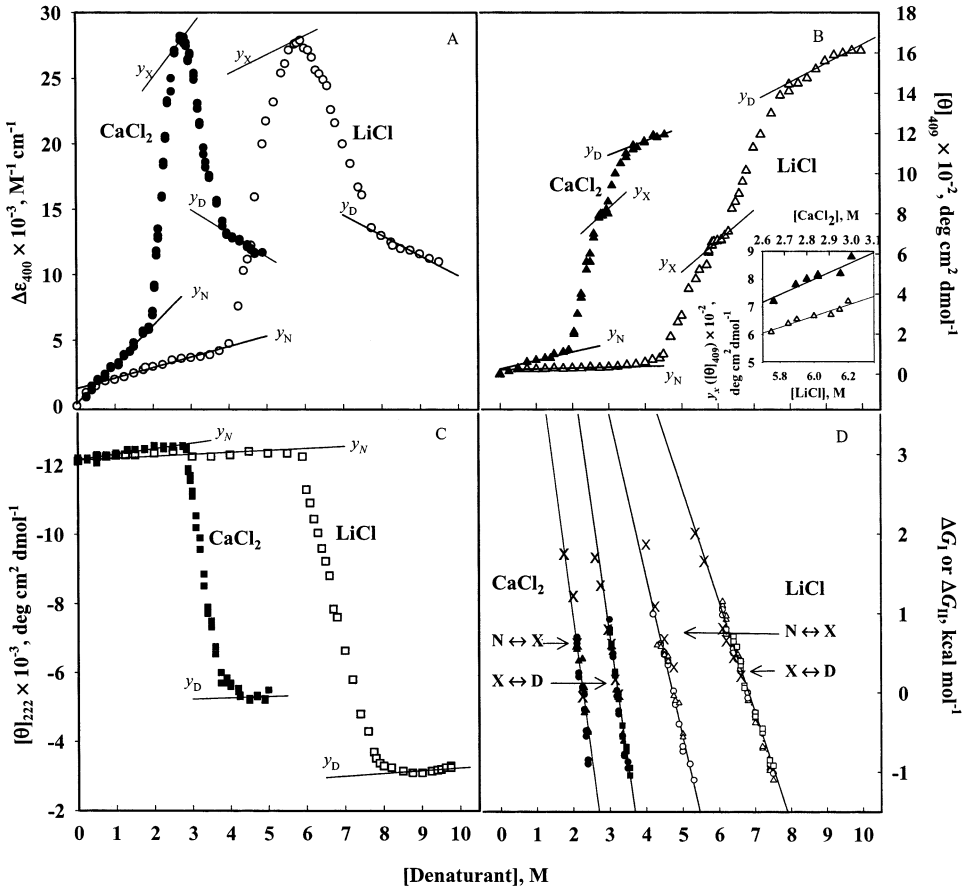

FIGURE 1: Equilibrium unfolding curves of h-cyt-c in the presence of LiCl (open symbols) and $CaCl_2$ (filled symbols) measured by $\Delta\epsilon_{400}$ (A), $[\theta]_{409}$ (B), and $[\theta]_{222}$ (C). See text for the dependence of y_x on [denaturant]. The inset in panel B shows the dependence of the optical property of the X state, y_x on [denaturant]. Panel (D) shows plots of ΔG_I and ΔG_{II} versus [denaturant]. In this panel X's are obtained from the studies of thermal denaturation in the presence of salt denaturants (see text), and other symbols have the same meaning as in panels A−C.

ized by far- and near-UV CD, intrinsic viscosity, and ANS−protein fluorescence measurements. We have also measured the heat-induced denaturation of both proteins in the presence of different concentrations of LiCl and $CaCl_2$. The thermal denaturation in the presence of the denaturants was monitored by the measurements of CD at 222 nm and absorption at 400 nm.

LiCl-Induced Denaturation at 25 ± 0.1 °C. Figure 1A shows the LiCl-induced transition of h-cyt-c followed by observing changes in $\Delta\epsilon_{400}$, which is a measure of the interaction between heme and globin molecules (*26*). This transition is a composite of at least two distinct processes. The first transition is centered in [LiCl] (molar concentration of LiCl) range 0−5.9 M and is represented here by the reaction N ↔ X, where X is the intermediate state of the protein between its N and D states. The second transition occurs in the [LiCl] range 6.0−10.0 M and is represented here by the reaction X ↔ D. It is seen in Figure 1A that the pretransition region occurs in a wide [LiCl] range, and as reported earlier (*27*), the optical property of the native protein, y_N shows nonlinear dependence on the [denaturant]. It should, however, be noted that the [LiCl] dependence of y_N (see the solid line in Figure 1A) is determined from the observed values of $\Delta\epsilon_{400}$ in the [LiCl] range 1.5−3.8 M. It is also seen in Figure 1A that the X state exists in a very narrow [LiCl] range, and the dependence of y_X, the optical property of the X state on [LiCl] cannot be determined from these results. As will be described later, we have determined [LiCl] dependence of y_X from the measurements of the heat-induced denaturation curves of h-cyt-c in the presence of LiCl in the concentration range 4.00−5.75 M (see inset in Figure 3A). The solid line shown in Figure 1A describes this dependence. As observed in the case of pretransition region, the posttransition region also occurs in a wide concentration range 8.0−10.0 M, and y_D, the property of the D state shows linear dependence on [LiCl] (see the solid line in Figure 1A). It has been observed that both transitions, N ↔ X and X ↔ D, are reversible.

Assuming that the process N ↔ X, designated here as transition I, follows a two-state mechanism, results shown in Figure 1A were used to determine values of ΔG_I (Gibbs energy change associated with the transition I) using the relation

$$\Delta G_I = -RT \ln [(y - y_N)/(y_X - y)] \qquad (3)$$

where R is the universal gas constant, T is the temperature in Kelvin, and y is the observed optical property corresponding to transition I. These values of ΔG_I in the range -1.3 kcal mol^{-1} $\leq \Delta G_I \leq$ 1.3 kcal mol^{-1} are plotted as a function of [denaturant] in Figure 1D. The plot of ΔG_I versus [LiCl] was analyzed for ΔG_I^0 (ΔG_I value at 0 M [denaturant]) and m_I, the slope ($\partial\Delta G_I/\partial$[denaturant]) using the relation (*28*)

$$\Delta G_I = \Delta G_I^0 - m_I[\text{denaturant}] \qquad (4)$$

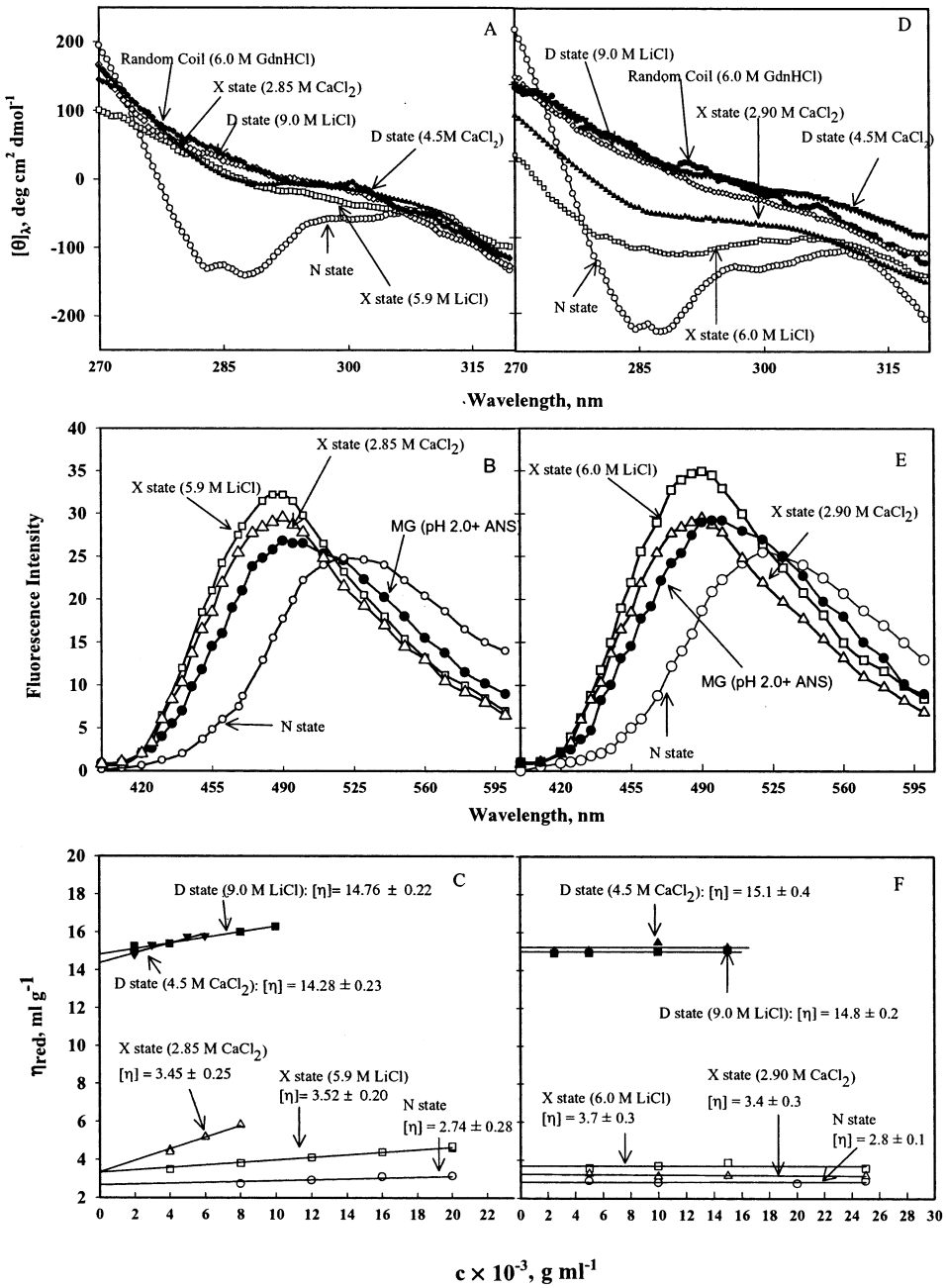

FIGURE 2: Near-UV CD spectra, fluorescence spectra in the presence of ANS, and intrinsic viscosity values in mL $g^{-1}$of the native (N), intermediate (X), and denatured (D) states at pH 6.0 and 25 °C. Panels A−C and D−F represent results of h-cyt-c and b-cyt-c, respectively. Molten globule (MG) florescence spectra of proteins at pH 2 in the presence of ANS are also shown in panels B and E.

The solid line was drawn according to eq 4 using values of ΔG_I^0 and m_I given in Table 1. This table also shows the value of $C_{m,I}$, the midpoint of transition I ($= \Delta G_I^0/m_I$).

Assuming that the process X ↔ D, designated here as transition II, is also of a two-state type, results shown in Figure 1A were used to determine values of ΔG_{II} (Gibbs energy change associated with the transition II) using the relation

$$\Delta G_{II} = -RT \ln [(y - y_X)/(y_D - y)] \quad (5)$$

where y is observed optical property corresponding to transition II. Values of ΔG_{II} in the range -1.3 kcal $mol^{-1} \leq \Delta G_{II}{}^1 \leq 1.3$ kcal mol^{-1} are plotted as a function of [LiCl] in Figure 1D, where it is seen that the plot of ΔG_{II} versus [denaturant] is linear. A linear least-squares analysis was used to obtain values of ΔG_{II}^0 and m_{II} using the relation

$$\Delta G_{II} = \Delta G_{II}^0 - m_{II}[\text{denaturant}] \quad (6)$$

where the subscript II represents the fact that these parameters correspond to transition II and the superscript "0" represents the value at 0 M LiCl. Values of ΔG_{II}^X, the value of ΔG_{II} at 5.9 M LiCl and $C_{m,II}$ ($= \Delta G_{II}^0/m_{II}$) were also determined.

Figure 1B shows the LiCl-induced transition curve of h-cyt-c followed by observing changes in $[\theta]_{409}$, the mean residue ellipticity at 409 nm, which is a probe for monitoring heme−globin interaction (*29*). As expected from the results shown in Figure 1A, this transition (Figure 1B) is also biphasic, i.e., it involves at least two distinct reactions, N ↔ X (transition I) and X ↔ D (transition II). Solid lines in

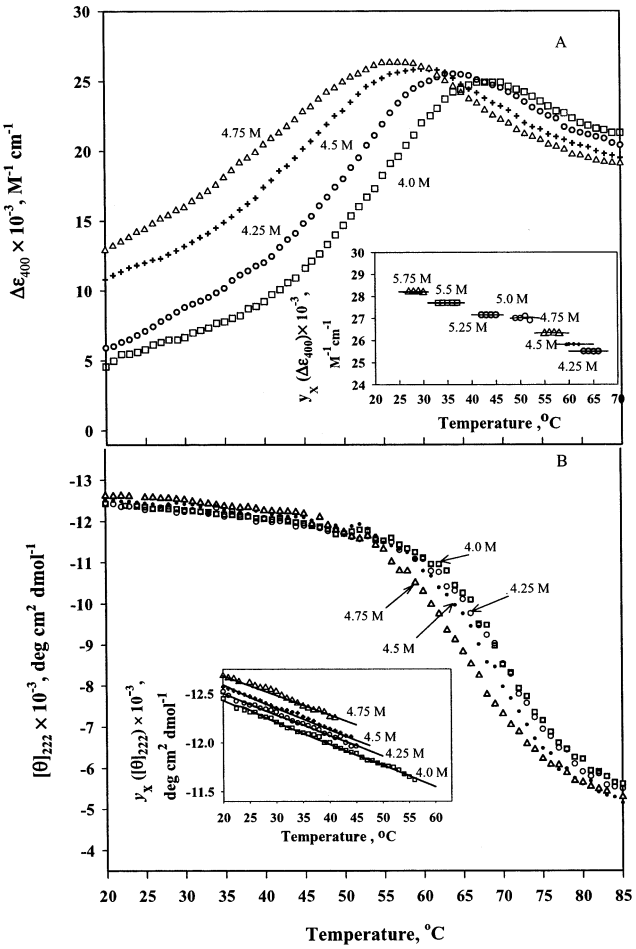

FIGURE 3: Thermal denaturation curves of h-cyt-c in the presence of 4.0, 4.25, 4.5, and 4.75 M LiCl monitored by $\Delta\epsilon_{400}$ (A) and $[\theta]_{222}$ (B). To maintain clarity transition curve in the presence of 5.0 M LiCl is not shown. Inset shows plots of y_X versus temperature at 4.25, 4.5, 4.75, 5.0, 5.25, 5.5, and 5.75 M LiCl.

Figure 1B show [LiCl] dependencies of the optical property of the native state, denatured state, and intermediate state. The inset in this figure shows data points that were used to determine the dependence of y_X on [denaturant].

Assuming that each transition follows a two-state mechanism, results shown in Figure 1B were used to determine values of ΔG_I and ΔG_{II} using eqs 3 and 5, respectively. The values of Gibbs energy change in the range -1.3 kcal mol^{-1} $\leq \Delta G \leq 1.3$ kcal mol^{-1} associated with each transition are plotted as a function of [LiCl] in Figure 1D. A linear least-squares analysis was used to analyze ΔG_I versus [LiCl] and ΔG_{II} versus [LiCl] plots for the thermodynamic parameters using eqs 4 and 6, respectively.

Figure 1C shows the LiCl-induced transition curve of h-cyt-c followed by observing changes in $[\theta]_{222}$, a measure of the secondary structure (*30*). A comparison of results shown in this figure with those shown in Figure 1A,B suggests that no change in secondary structure occurs during the transition between N and X states. It is also seen in this figure that unfolding of the secondary structure occurs in the [LiCl] range 6.0−9.0 M, which corresponds to the transition X ↔ D (see Figure 1A,B). Assuming that the transition X ↔ D monitored by $[\theta]_{222}$ measurements is of a two-state type, values of ΔG_{II} were determined at different LiCl concentrations using eq 5. The ΔG_{II} versus [LiCl] plot is shown in Figure 1D. A least-squares analysis of this plot according to eq 6 gave values of thermodynamic parameters.

Figure 2A shows the near-UV CD spectra of h-cyt-c in the native, intermediate, and denatured states. It can be seen in this figure that the near-UV CD spectrum of the X state is similar to that of the D state, and the characteristic negative peaks in the region 282−289 nm of the native protein that arise from the tryptophan and tyrosyl side-chains (*7*, *31*) are absent in both X and D states. Figure 2A also shows the CD spectrum of the randomly coiled h-cyt-c in 6 M guanidine hydrochloride (GdnHCl), which is identical to those of X and D states observed in the presence of LiCl.

Figure 2B shows the ANS fluorescence when it is added to h-cyt-c in the native and X states. The excitation was carried out at 365 nm and emission was recorded in the range 400−600 nm. It is seen in Figure 2B that the fluorescence of ANS, in the presence of the protein existing in the X state, shows an increase in fluorescence intensity accompanied by a blue shift with respect to native state. It should be noted that the fluorescence measurements in the presence of LiCl concentration that gives the D state cannot be carried out due to the insolubility of ANS in high denaturant concentrations.

Figure 2C shows the reduced viscosity, η_{red}, of h-cyt-c in the native, intermediate, and denatured states as a function of protein concentration. A linear least-squares analysis of the plot of η_{red} versus c, the protein concentration, gave the value of the intrinsic viscosity ($[\eta]$), the value of η_{red} at $c = 0$ (*32*). It can be seen in Figure 2C that the value of $[\eta]$ increases from 2.74 ± 0.28 mL g^{-1} for the native protein to values of 3.52 ± 0.20 mL g^{-1} for the X state and 14.76 ± 0.22 mL g^{-1} for the D state. A comparison of $[\eta]$ of the D state with that of the protein in 6 M GdnHCl ($[\eta] = 14.5$ ml g^{-1}) (*17*, *24*) suggests that h-cyt-c in concentrated LiCl solution behaves as a random coil.

Effect of Temperature on N ↔ X Equilibrium. We have studied the effect of temperature on h-cyt-c in the presence of LiCl in the concentration range 4−5 M in which N ↔ X equilibrium exists at 25 °C (see Figure 1A). It has been observed that the thermal denaturation of the protein is reversible at all LiCl concentrations. Figure 3A shows typical heat-induced transition curves in this [LiCl] range. It is seen in this figure that h-cyt-c in the presence of a fixed [LiCl] undergoes a biphasic transition. However, the transition occurring in the higher temperature range is not complete even at 85 °C. To understand the nature of each of these transitions, heat-induced unfolding of h-cyt-c in the identical denaturing conditions was also measured by monitoring change in $[\theta]_{222}$. Figure 3B shows typical results of these measurements. It is seen in this figure that the pretransition baseline shows dependence on both T and [LiCl]. The inset in this figure shows results that were used to determine this dependence. Figure 3B also shows that the heat-induced denaturation is incomplete at LiCl concentrations in the measurable temperature range. At each [LiCl], a comparison of the thermal transition curve measured by $\Delta\epsilon_{400}$ (Figure 3A) with that followed by $[\theta]_{222}$ measurements (Figure 3B) suggests (i) that no change in $[\theta]_{222}$ occurs in the lower temperature range in which transition N ↔ X is observed during $\Delta\epsilon_{400}$ measurements, and (ii) that the second transition monitored by $\Delta\epsilon_{400}$ measurements represents the melting of the secondary structure.

Table 1: Thermodynamic Parameters Characterizing the LiCl and $CaCl_2$ Denaturations of h-cyt-c and b-cyt-c at pH 6.0 and 25 °C[a]

		h-cyt-c			b-cyt-c		
denaturant	transition	$\Delta G_I^0/\Delta G_{II}^{X_b}$ kcal mol^{-1}	m_I/m_{II} kcal mol^{-1}	C_{mI}/C_{mII} M	$\Delta G_I^0/\Delta G_{II}^{X_a}$ kcal mol^{-1}	m_I/m_{II} kcal mol^{-1}	C_{mI}/C_{mII} M
LiCl	N ↔ X	9.5 ± 0.3	−2.0 ± 0.1	4.8 ± 0.1	10.5 ± 0.2	−2.1 ± 0.1	5.1 ± 0.2
	X ↔ D	1.5 ± 0.3	−1.5 ± 0.1	6.7 ± 0.1	1.5 ± 0.4	−1.9 ± 0.1	6.8 ± 0.2
$CaCl_2$	N ↔ X	9.2 ± 0.4	−4.1 ± 0.1	2.3 ± 0.1	10.3 ± 0.4	−4.5 ± 0.1	2.3 ± 0.1
	X ↔ D	1.2 ± 0.3	−3.4 ± 0.2	3.2 ± 0.1	0.9 ± 0.1	−3.6 ± 0.1	3.1 ± 0.1

[a] Since for each transition induced by given denaturant, (ΔG, [denaturant]) data obtained from different optical probes fall on the same line, all data were taken together to get the best fit according to eq 4 for N ↔ X and eq 6 for X ↔ D transitions. [b] ΔG_{II}^X is the value of ΔG_{II} at [denaturant] where the X state exists.

Assuming that the first transition curve of h-cyt-c at a given [LiCl] shown in Figure 3A, represents a two-state process N ↔ X (transition I), one can determine ΔG_I as a function of temperature using eq 3, provided the temperature dependencies of y_N and y_X are known at each [LiCl]. Inset of Figure 3A shows plots of $\Delta\epsilon_{400}$ of the protein in the X state as a function of temperature at different LiCl concentrations. It is seen in this figure that y_x can be observed in a very narrow temperature range, it does not depend on temperature, and it shows dependence on [LiCl]. The relation describing this [LiCl] dependence of y_X was determined, and it was used to draw the solid line showing the y_x dependence on [LiCl] in Figure 1A. To determine the dependency of y_N of cyt-c on composition variables ([LiCl] and temperature), the native protein was heated at 1.5, 2.0, 3.0, and 3.5 M of LiCl, and $\Delta\epsilon_{400}$ was measured as a function of temperature. It was observed that y_N depends on both temperature and [LiCl]. Using these observations on y_N, y_X, and values of y ($\Delta\epsilon_{400}$) of the heat-induced transition between N and X states (Figure 3A), ΔG_I was determined at each temperature with the help of eq 3. At each [LiCl] value of ΔG_I in the range -1.3 kcal mol$^{-1} \leq \Delta G_I \leq 1.3$ kcal mol^{-1} in the transition region were plotted against temperature, and these plots (stability curves not shown) were analyzed to determine the value of $T_{m,I}$, the midpoint of transition I and $\Delta H_{m,I}$, the enthalpy change at $T_{m,I}$, using the procedure described earlier (*33*). Values of $\Delta H_{m,I}$ and $T_{m,I}$ at different LiCl concentrations are shown in Figure 4A. A linear least-squares analysis of $\Delta H_{m,I}$ versus $T_{m,I}$ plot gave the value of 0.90 ± 0.08 kcal mol^{-1} K^{-1} for $\Delta C_{p,I}$, the constant-pressure heat capacity change ($= (\partial\Delta H_{m,I}/\partial T_{m,I})_p$) associated with N ↔ X process (transition I) induced by LiCl. Values of $T_{m,I}$, $\Delta H_{m,I}$, and $\Delta C_{p,I}$ were used for determining ΔG_I at a given [LiCl] and 25 °C using the relation

$$\Delta G_I = \Delta H_{m,I}[(T_{m,I} - 298)/T_{m,I}] - \Delta C_{p,I}[T_{m,I} - 298 + 298\ln(298/T_{m,I})] \quad (7)$$

values of ΔG_I at 25 °C thus determined are represented by X's in Figure 1D.

Effect of Temperature on X ↔ D Equilibrium. We have measured the heat-induced denaturation curves (plot of $\Delta\epsilon_{400}$ versus temperature) of h-cyt-c in the presence of LiCl concentration range 6.0−6.8 M in which the protein exhibits X ↔ D equilibrium at 25 °C (see Figure 1A). It has been observed that the thermal denaturation of the protein is reversible at all LiCl concentrations. Figure 5A shows typical denaturation curves of these measurements. It can be seen in this figure that the optical property of the denatured protein, y_D, shows dependence on temperature and [LiCl]. The relations describing this temperature dependence of y_D at different denaturant concentrations were determined.

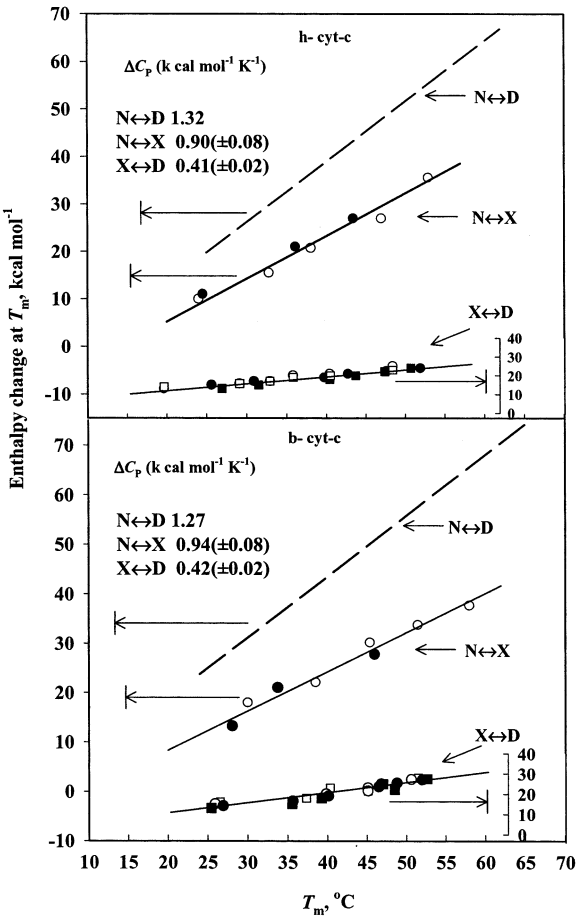

FIGURE 4: ΔH_m versus T_m plots of h-cyt-c and b-cyt-c in the presence of various concentrations of LiCl (open symbols) and $CaCl_2$ (filled symbols). For transition N ↔ X of both proteins, LiCl and $CaCl_2$ concentrations are 4.0, 4.25, 4.5, 4.75, and 5.0 M and 2.0, 2.1, and 2.25 M, respectively. For transition X ↔ D of both proteins, LiCl and $CaCl_2$ concentrations are 6.0, 6.2, 6.4, 6.6, and 6.8 M and 2.75, 2.85, 2.95, 3.05, 3.15, and 3.25 M, respectively. Circles and squares represent (ΔH_m, T_m) data obtained from $\Delta\epsilon_{400}$ and $[\theta]_{222}$ measurements, respectively. Broken lines represent enthalpies at midpoint temperature for N ↔ D process in the pH range 2.0−6.5 (*41*, *44*).

We have also monitored the heat-induced denaturation of h-cyt-c in the presence of LiCl concentration range 6.0−6.8 M by measuring CD at 222 nm and observed that the thermal denaturation of the protein is reversible at each [LiCl]. Typical denaturation transitions are shown in Figure 5B. It can be seen in this figure that y_D ($[\theta]_{222}$ of the D state) shows

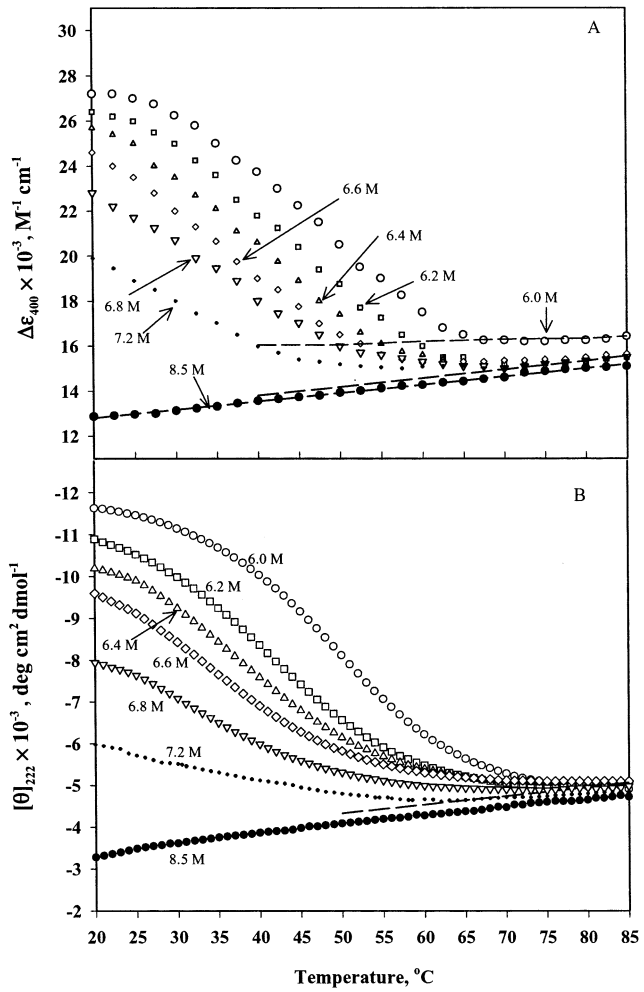

FIGURE 5: Thermal denaturation curves of h-cyt-c in the presence of 6.0, 6.2, 6.4, 6.6, 6.8, and 8.2 M LiCl monitored by $\Delta\epsilon_{400}$ (A) and $[\theta]_{222}$ (B) measurements.

dependence on both T and [LiCl]. The relation describing the y_D dependence on temperature and [LiCl] was determined. It should be noted that these dependencies of $[\theta]_{222}$ of D states on the composition variables ([LiCl] and T) were determined using data in the same [LiCl] ranges as used in the case of $\Delta\epsilon_{400}$ measurements.

Assuming that heat-induced denaturation (transition II) of h-cyt-c in the presence of LiCl follows a two-state mechanism, each transition curve presented in Figure 5A,B was analyzed for ΔG_{II}, at each temperature and [LiCl] using eq 5 with known dependencies of y_x and y_D on [LiCl] and T. We have constructed stability curves (ΔG_{II} versus T) at all LiCl concentrations (plots not shown) and analyzed these plots for $\Delta H_{m,II}$ and $T_{m,II}$ values. Values of these thermodynamic parameters are shown in Figure 4A. A linear-least-squares analysis of $\Delta H_{m,II}$ versus $T_{m,II}$ plot gave a value of 0.41 (± 0.02) kcal mol^{-1} K^{-1} for $\Delta C_{p,II}$. At a given [LiCl], values of $T_{m,II}$, $\Delta H_{m,II}$, and $\Delta C_{p,II}$ were used for determining ΔG_{II} at 25 °C using eq 8, and these values are shown as X's in Figure 1D.

$$\Delta G_{II} = \Delta H_{m,II}[(T_{m,II} - 298)/T_{m,II}] - \Delta C_{p,II}[T_{m,II} - 298 + 298 \ln(298/T_{m,II})] \quad (8)$$

$CaCl_2$-Induced Denaturation at 25 ± 0.1 °C. Figure 1 shows $CaCl_2$-induced denaturation curves of h-cyt-c at pH 6.0 at 25 °C, followed by observing changes in $\Delta\epsilon_{400}$ (panel A), $[\theta]_{409}$ (panel B), and $[\theta]_{222}$ (panel C). It is seen in this figure that, as observed in the case of LiCl-induced denaturation of the protein, $CaCl_2$ induces a biphasic transition when unfolding of the protein was followed by observing changes in $\Delta\epsilon_{400}$ and $[\theta]_{409}$, whereas single step unfolding was observed in case of $[\theta]_{222}$ measurements. The $CaCl_2$-induced denaturation was reversible. Denaturation curves were analyzed for thermodynamic parameters associated with transitions N ↔ X and X ↔ D using eqs 3−6 in a manner similar to that used for the analysis of LiCl-induced transition curves. Values of thermodynamic parameters for transition I and transition II are given in Table 1.

The intermediate X observed on the denaturation pathway, N ↔ X ↔ D, has been characterized by far-UV CD measurements (Figure 1C), near-UV CD measurements (Figure 2A), ANS−protein fluorescence intensity measurements (Figure 2B), and $[\eta]$ measurements (Figure 2C). It can be seen in these figures that the structural characteristics of the X state in the presence of $CaCl_2$ are the same as those observed for the state X in the presence of LiCl (Figure 2A−C). It should be noted that fluorescence measurements in the presence of $CaCl_2$ concentration that gives the D state could not be carried out due to the insolubility of ANS in the high denaturant concentrations.

Effect of Temperature on $CaCl_2$-Induced Denaturation of h-cyt-c. We have also studied the effect of temperature on N ↔ X and X ↔ D equilibria induced by $CaCl_2$ by measuring changes in $\Delta\epsilon_{400}$ and $[\theta]_{222}$. It was observed that the thermal unfolding followed by $\Delta\epsilon_{400}$ measurements induces a reversible biphasic transition; transition I in $[CaCl_2]$ range 2.0−2.6 M and transition II at concentrations above 2.8 M. On the other hand, the thermal unfolding transition followed by $[\theta]_{222}$ at various denaturant concentrations showed a simple single-step denaturation process. These results are similar to those obtained for the thermal unfolding of the protein at different concentrations of LiCl. The method employed to analyze the thermal unfolding transition curves was the same as the one used for analyzing thermal denaturation curves shown in Figures 3 and 5. Results of this analysis are given in Figure 4A.

To see the effect of amino acid substitution on h-cyt-c denaturation process and on the thermodynamic parameters associated with denaturation, we have carried out identical sets of experiments on b-cyt-c, which differs from its horse homologue in three helical amino acid residues (*34*). Figure 6 (panels A−C) shows reversible LiCl- and $CaCl_2$-induced denaturations of b-cyt-c monitored by observing changes in $\Delta\epsilon_{400}$, $[\theta]_{409}$, and $[\theta]_{222}$ at pH 6.0 and 25 °C. $\Delta\epsilon_{400}$ and $[\theta]_{409}$ measurements suggest that the unfolding by both denaturants is biphasic and involves the formation of an intermediate (Figure 6A,B), whereas $[\theta]_{222}$ measurements give a single transition between N and D states (Figure 6C). The intermediate state obtained in the presence of low concentrations of these denaturants that retains all the native secondary structure (see Figure 6C) was characterized by the near-UV CD, ANS−protein fluorescence, and intrinsic viscosity measurements. Figure 2D shows the near-UV CD spectra of the protein in the native, intermediate, and denatured states. It is seen in this figure that the near-UV CD spectra of the D state obtained in the presence of LiCl and $CaCl_2$ are comparable to that of the random coil protein. It can

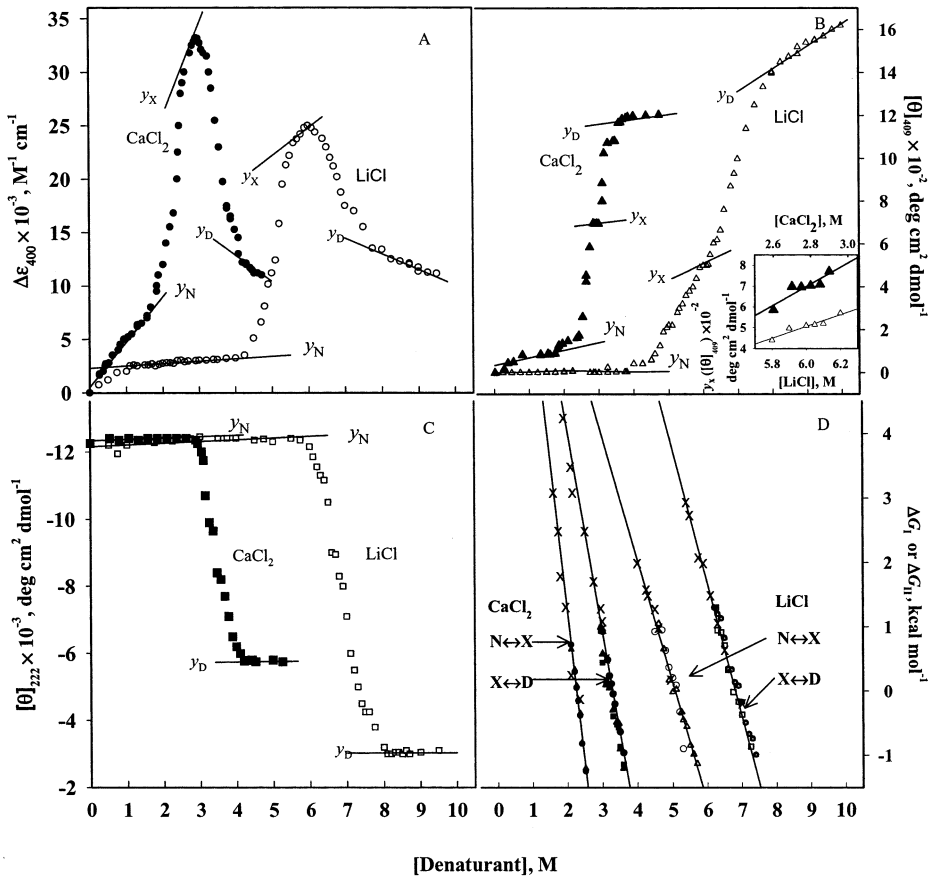

FIGURE 6: LiCl (open symbols) and $CaCl_2$ (filled symbols) denaturations of b-cyt-c at pH 6.0 and 25 °C, measured by $\Delta\epsilon_{400}$ (A), $[\theta]_{409}$ (B), and $[\theta]_{222}$ (C). Panel (D) shows plots of ΔG_I and ΔG_{II} versus [denaturant]. In this panel, X's are obtained from the studies of thermal denaturation in the presence of salt denaturants (see text), and other symbols have the same meaning as in panels A−C.

also be seen in this figure that the characteristic negative peaks in the region 282−289 nm of the native protein (*31*) are absent in the X state in the presence of low concentrations of LiCl and $CaCl_2$. Figure 2E shows the ANS fluorescence in the presence of b-cyt-c in the native and X states. As we did in the case of h-cyt-c, the excitation was carried out at 365 nm and emission spectrum was recorded in the range 400−600 nm. It can be seen in Figure 2E that the fluorescence of ANS in the presence of the protein existing in the X state shows an increase in fluorescence intensity accompanied by a blue shift. It should be noted that fluorescence measurements in the presence of LiCl or $CaCl_2$ concentrations that give the D state could not be carried out due to the insolubility of ANS in the high denaturant concentrations.

Figure 2F shows the measurements of $[\eta]_{red}$ of b-cyt-c in the native, intermediate, and denatured states as a function of protein concentration. A linear least-squares analysis gave $[\eta]$ (mL g^{-1}) values of 2.8 ± 0.1 for the N state, 3.7 ± 0.3 (LiCl) and 3.4 ± 0.3 ($CaCl_2$) for the X state and 14.8 ± 0.2 (LiCl) and 15.1 ± 0.4 ($CaCl_2$) for the D state.

Since the unfolding process of b-cyt-c by LiCl and $CaCl_2$ (Figure 6A−C) is similar to that of the denaturation path followed by h-cyt-c (Figure 1A−C), we have analyzed these denaturation curves for thermodynamic parameters in a manner identical to the one used for the analysis of denaturation curves shown in Figure 1A−C. Values of these parameters are given in Table 1.

As we did in the case of h-cyt-c, we have studied the effect of heat on LiCl- and $CaCl_2$-induced denaturation of b-cyt-c by monitoring changes in $\Delta\epsilon_{400}$ and $[\theta]_{222}$. It has been observed that the heat-induced denaturation of the protein in the presence of LiCl (4.0, 4.25, 4.5, 4.75, 5.0, 6.0, 6.2, 6.4, 6.6, and 6.8 M) and $CaCl_2$ (2.0, 2.1, 2.25, 2.75, 2.85, 2.95, 3.05, 3.15, and 3.25 M) is reversible. We have analyzed thermal denaturation curves of b-cyt-c for thermodynamic parameters, i.e., T_m, ΔH_m, and ΔC_p using same procedure as used in the case of h-cyt-c. Values of T_m and ΔH_m in the presence of different concentrations of both denaturants and ΔC_p values are given in Figure 4B.

DISCUSSION

The denaturation of horse and bovine cyts-c by weak inorganic salt denaturants (LiCl and $CaCl_2$) monitored by $\Delta\epsilon_{400}$ and $[\theta]_{409}$ measurements is a biphasic (N ↔ X↔ D) process (see Figures 1A,B and 6A,B). This equilibrium study of denaturation provides a direct evidence of the presence of a stable folding intermediate at neutral pH, which gets populated in extremely narrow range of the denaturant concentration. For each protein, a comparison of the denaturation curves monitored by $\Delta\epsilon_{400}$ and $[\theta]_{409}$ with that monitored by $[\theta]_{222}$ reveals that there is no change in the peptide CD in the denaturant concentration range where transition I (N ↔ X) is observed (see Figures 1A−C and 6A−C). This comparison suggests that the intermediate state X has one of the structural characteristics of the molten globule state, namely, the presence of almost all the secondary structure that the native protein originally had (*1*). To ascertain whether the X state has other molten globule-like characters, we have carried out fluorescence measure-

ments of ANS in the presence of horse and bovine proteins, for ANS shows increase in fluorescence intensity with a blue shift in the emission maximum on binding with exposed hydrophobic clusters which are known to be present in the molten globule (*1*, *35*). Our observations suggest that the fluorescence intensity and wavelength maximum of ANS emission spectrum are unperturbed in the presence of both native proteins, whereas there is a significant change in the intensity and a blue shift in the emission maximum of ANS in the presence of the protein in the X state (see Figure 2). These results suggest that the X state has a molten globule characteristic, namely, loosely packed hydrophobic core that increases the hydrophobic surface accessible to solvent (*1*, *35*, *36*). Another known structural characteristic of the molten globule is the absence of most of the specific tertiary structure produced by tight packing of the side chains in the native protein (*37*, *38*). The near-UV CD spectral measurements of horse cyt-c show that the characteristic native interactions are completely lost in the X state, for the CD spectra of the X state in both denaturants, are within experimental errors, identical to that of the randomly coiled state (see Figure 2B). Furthermore, a comparison of these CD spectra with those of the molten globule of h-cyt-c reported earlier (*37*) also suggests that the intermediate state X is a molten globule. A comparison of the near-UV CD spectra of the X state of b-cyt-c with those of the N and D states of the protein suggests that the characteristic native tertiary interactions are only partially lost in the X state (see Figure 2D). This finding is consistent with the reports that there is remarkable diversity among the molten globule states of homologous proteins, and there is substantial native-like tertiary packing in molten globule of some proteins (*1*). To further characterize the X state, intrinsic viscosity of N, X, and D states of bovine and horse cyts-c were measured under appropriate experimental conditions (see Figure 2C,F). These measurements show that $[\eta]$ of the X state is about 20−25% more than that of the native state. That is, the compactness of the X state in terms of radius of gyration is about 10−15% more than that of the native state. It is interesting to note that the increase in the radius of gyration of h-cyt-c is about 26% (*39*) upon the transition from native to the MG state at pH 2. One possible explanation for the smaller value of the radius of gyration of MG observed here, could be because h-cyt-c (pI = 10.7) will be more expanded at pH 2 than at pH 6. We conclude that the intermediate state X of the folding ↔ unfolding reaction of bovine and horse cyts-c induced by LiCl or $CaCl_2$ has all the common structural characteristics of the molten globule state (*1*).

The molten globule state of the protein is not only structurally quite different from the unfolded and native states, but also represents a new thermodynamic state, in addition to the previously known native and denatured states (*1*). It has been shown by a number of authors that the heat capacity of the molten globule state is significantly larger than that of the native state (for a review see ref *40*). We have determined ΔC_p of cyts-c associated with the processes N ↔ X (molten globule) and X ↔ D and obtained, respectively, values of 0.90 (± 0.08) and 0.41 (± 0.02) kcal mol^{-1} K^{-1} for h-cyt-c and 0.94 (± 0.08) and 0.42 (± 0.02) kcal mol^{-1} K^{-1} for b-cyt-c (see Figure 4). It is seen in Figure 4 that sum of these values of ΔC_p for transitions I and II of each protein are in excellent agreement with that obtained by DSC measurements for the process N ↔ D (*40*, *41*). The structural and thermodynamic characterizations of the molten globule states of bovine and horse cyts-c permit us to conclude that this state is stabilized by both secondary structure and hydrophobic interactions.

Many authors have reported that the acid denatured h-cyt-c can regain almost all native secondary structure on addition of (i) neutral salts (*4*, *38*, *42*), (ii) low concentrations of GdnHCl (*9*), (iii) ANS (*8*), and (iv) sugar (*43*). The molten globule thus formed has the intrinsic viscosity of 3.5 mL g^{-1} (*4*), the radius of gyration of 17−20 Å (*5*, *39*), nonpolar groups exposed to solvent (*4*, *5*, *42*, *43*) and ΔC_p of 0.3−0.4 kcal mol^{-1} K^{-1} (*7*, *9*) for the process MG conformation ↔ D conformation. These structural and thermodynamic characteristics of the molten globule state of h-cyt-c at pH 2 are comparable to those observed here in the presence of low concentrations of LiCl and $CaCl_2$ near neutral pH.

To analyze N ↔ X ↔ D transition for thermodynamic parameters of bovine and horse cyts-c at 25 °C, two assumptions, namely, a two-state mechanism of LiCl- and $CaCl_2$-induced denaturations and a linear dependence of ΔG_D on [denaturant] were introduced. One of the criteria to test the validity of a two-state transition is to see whether one gets comparable values of thermodynamic parameters associated with the transition curve monitored by different structural probes. It can be seen in Figures 1D and 6D that, for each transition of both proteins, values of ΔG from different optical methods fall on the same ΔG versus [denaturant] plot, suggesting that a two-state assumption seems to be valid. A more authentic test for the validity of the two-state assumption is to compare the total Gibbs free energy change associated with N ↔ X ↔ D observed here with that from the DSC measurements for a two-state N ↔ D transition. It is interesting to note that the values of calorimetric Gibbs free energy change for N ↔ D transitions, which are 10 and 11 kcal mol^{-1} for h-cyt-c and b-cyt-c (*41*, *44*), respectively, are in excellent agreement with those ($\Delta G_I^0 + \Delta G_{II}^X$) obtained from optical methods (see Table 1). Thus, a two-state assumption for N ↔ X and X ↔ D at pH 6.0 and 25 °C is valid. Another assumption that ΔG_D is linear function of the [denaturant] seems to be justified, for values of ΔG_I (or ΔG_{II}) estimated for the heat-induced denaturation of protein in the presence of LiCl and $CaCl_2$ fall on the same line drawn from the denaturation results obtained at 25 °C (see X's in Figures 1D and 6D).

It can be seen in Table 1 that about 85% of the total Gibbs energy change is associated with N ↔ X transition. This is an important observation, for it suggests that the stability of native protein is mainly due to interactions that are absent in molten globule state. As discussed above, the molten globule state of cyts-c is devoid of tight packing of the hydrophobic side chains, which play a role in the stabilization of the native state (*45*). It has been shown that the covalently bound heme interacts with about 35% of the buried side chains (*46*), and that the removal of heme from cyt-c leads to unfolding of the polypeptide backbone (*47*). Thus, the packing of hydrophobic side chains and heme play a dominant role in stabilizing the native state of cyts-c. Furthermore, contribution to native stability due to the presence of secondary structure seems to be very small.

The heat capacity measurements show that ΔC_p of the molten globule (X) state of cyts-c is intermediate between those of the native and unfolded states. It amounts to about 70% of the total difference between the native and unfolded states. Because the positive ΔC_p associated with protein unfolding is known to be associated with the exposure of the hydrophobic groups to water, this observation is consistent with the notion that MG retains a part of the native hydrophobic core devoid of water molecules, and the hydrophobic interactions are also important in the stabilization of molten globules (*40*). Furthermore, the MG state of cyts-c retains all the secondary structure present in the native protein (Figures 1 and 6). These results led us to conclude that the MG state of cyt-c is stabilized by hydrophobic interactions and secondary structure.

The nature of the unfolding transition between molten globule and unfolded states has not yet been well understood, for it is noncooperative for some proteins (*48*) and a highly cooperative and two-state type for others (*7*, *49*). The salt denaturant-induced denaturation measurements at 25 °C (Figures 1 and 5) and heat-induced denaturation measurements in the presence of appropriate concentrations of LiCl and $CaCl_2$ (e.g., see Figure 3) suggest that the unfolding transition of the molten globule state of bovine and horse cyts-c is highly cooperative and reversible. As discussed above, all the pieces of evidence obtained here suggest that the transition between MG and D states of h-cyt-c and b-cyt-c follows a two-state mechanism at 25 °C. That the heat-induced MG ↔ D process of each protein is also a two-state process is evident from the coincidence of thermodynamic parameters obtained from $\Delta\epsilon_{400}$ and $[\theta]_{222}$ measurements (Figure 4) and from the excellent agreement between $\Delta C_{p,II}$ values (Figure 4) and calorimetric ΔC_p, associated with thermal unfolding of MG (*9*, *50*); $\Delta C_{p,II}$ values of horse and bovine proteins are 0.41 ± 0.03 and 0.42 ± 0.04 kcal mol^{-1} K^{-1}, respectively, and the calorimetric ΔC_p for the thermal unfolding of the MG state is 0.4 kcal mol^{-1} K^{-1} for h-cyt-c (*9*, *50*). Extrapolation of $\Delta H_{m,II}$ and $T_{m,II}$ versus [denaturant] plots (not shown) to the concentrations of a denaturant in which the protein exists in the MG state gave, respectively, values of 28 ± 4 kcal mol^{-1} and 49.8 ± 0.5 °C for $\Delta H_{m,II}$ and $T_{m,II}$, for h-cyt-c and 30 ± 2 kcal mol^{-1} and 50.3 ± 0.5 °C for $\Delta H_{m,II}$ and $T_{m,II}$ for b-cyt-c. These values are in very good agreement with those obtained from DSC measurements; the calorimetric values are $\Delta H_m \sim 35$ kcal mol^{-1} and $T_m \sim 50$ °C (*9*, *50*, *51*). Using values of $\Delta H_{m,II}$, $T_{m,II}$ and $\Delta C_{p,II}$ in eq 8, we obtained ΔG_{II}^X values of 1.2−1.5 and 1.1−1.4 kcal mol^{-1} at 25 °C for h- and b-cyts-c, respectively. These values of Gibbs energy change are in excellent agreement not only with those obtained from isothermal unfolding (see Table 1) but also with calorimetric value of 1.33 kcal mol^{-1} at 25 °C (*9*). We conclude that the MG state obtained in the presence of LiCl and $CaCl_2$ at pH 6 and 25 °C is thermodynamically indistinguishable from that obtained at low pH in the presence of stabilizing cosolvents and acetylation of lysine residues of cyt-c (*9*).

Contrary to MG ↔ D transition, thermodynamic parameters associated with N ↔ MG of cyt-c have not been experimentally determined. However, these were predicted from the difference between the values of the parameter for N ↔ D transition and for MG ↔ D transition. The predicted values of h-cyt-c from DSC measurements are $\Delta G_D^\circ = 8.5-8.7$ kcal mol^{-1}, $\Delta H_m = 70-80$ kcal mol^{-1}, $\Delta C_p = 0.9-1.05$ kcal mol^{-1} K^{-1} (*7*). (No such studies are reported from bovine protein.) We have determined the values of thermodynamic parameters associated with the process N ↔ MG from the reversible heat-induced denaturation of the protein in the presence of LiCl and $CaCl_2$. Values of $\Delta C_{p,I}$ of both proteins given in Figure 4 are in excellent agreement with those predicted from the calorimetric measurements (*7*, *9*, *50*). Values of of $\Delta H_{m,I}$ and $T_{m,I}$ in different concentrations of LiCl and $CaCl_2$ and that those of $\Delta C_{p,I}$ are shown in Figure 4. For a protein in a given denaturant, value of ΔG_{II} were estimated using eq 7 with the values of $\Delta H_{m,I}$ and $T_{m,I}$ and $\Delta C_{p,I}$ shown in this figure, and ΔG_I values were plotted against [denaturant]. The extrapolation of such a plot to 0 M denaturant concentration gave values of ΔG_I^0, the Gibbs energy of stabilization, of 9.01 ± 0.7 and 10.2 ± 0.5 kcal mol^{-1} for the h-cyt-c and b-cyt-c, respectively. These ΔG_I^0 values associated with N ↔ MG transition of proteins are in excellent agreement with those obtained from isothermal measurements as well (Table 1). Furthermore ΔG_I^0 of h-cyt-c is in good agreement with that obtained by DSC measurements (*7*). To compare the calorimetric ΔH_m with our values we have determined values of $\Delta H_{m,I}^0$, the value of $\Delta H_{m,I}$ in the absence of the denaturant from the extrapolation of the plot of $\Delta H_{m,I}$ versus [denaturant] to 0 M denaturant. The extrapolated values are 86 ± 6 and 92 ± 7 kcal mol^{-1} for $\Delta H_{m,I}^0$ of h-cyt-c and b-cyt-c, respectively, which are in good agreement with those predicted from the DSC measurements.

Folding of a protein in vitro is likely to differ in many details from that in the cell. However, one feature, which is common in both in vitro and in vivo folding, is the existence of the MG state on the folding ↔ unfolding pathway (*1*, *52*). In vitro experiments have shown that acid-denatured cyt-c is transformed into the MG state on the addition of several additives (*5*, *8*, *38*). However, there exists no evidence to show the formation of the native state of cyt-c from its MG state that exists at low pH. On the other hand, the MG state that has been observed in this study near neutral pH reversibly folds to the native state. Thus, our work on the characterization of the MG state of cyts-c is expected to have a more physiological relevance than the earlier studies of characterization of the MG state of the protein at low pH.

Finally, on the basis of the results obtained in this study it is possible to conclude that (i) the thermodynamically stable intermediate on the reversible folding ↔ unfolding pathway has all the common structural characteristics of the molten globule; (ii) although the MG state of proteins retain the entire native helical structure, it is only marginally more stable than the unfolded protein; and (iii) the hydrophobic interaction is important in stabilizing the molten globule state of proteins, for the MG state retains a part of the native hydrophobic core devoid of water molecules.

ACKNOWLEDGMENT

We thank Dr. W. Pfeil (Potsdam University, Potsdam, Germany) for a critical reading of the manuscript. We also thank Dr. M. A. Baig (Hamdard University, New Delhi, India) for his help with the fluorescence measurements.

SUPPORTING INFORMATION AVAILABLE

(a) Dependence of optical properties of the native, molten globule and denatured states of cytochromes-c on [denaturant] and temperature. (b) Thermodynamic parameters (ΔG, m, C_m) of proteins obtained from the transition curves measured by each of the optical properties ($\Delta\epsilon_{400}$, $[\theta]_{409}$, and $[\theta]_{222}$) at pH 6.0 and 25 °C. (c) Thermal denaturation curves of h-cyt-c in the presence of different concentrations of $CaCl_2$, monitored by $\Delta\epsilon_{400}$ and $[\theta]_{222}$ measurements. (d) Thermal denaturation curves of b-cyt-c in the presence of different concentrations of LiCl and $CaCl_2$ monitored by $\Delta\epsilon_{400}$ and $[\theta]_{222}$ measurements. This material is available free of charge via the Internet at http://pubs.acs.org.

REFERENCES

1. Arai, M., and Kuwajima, K. (2000) Role of the molten globule state in protein folding. *Adv. Protein Chem. 53*, 209−271.
2. Das, B. K., Bhattacharyya, T., and Roy, S. S. (1995) Characterization of a urea-induced intermediate state of glutamyl- t-RNA synthase from *E. coli*. *Biochemistry 34*, 5242−5247.
3. Oghasahara, K., Matsushita, E., and Yatuni, K. (1993) Further examination of intermediate state in the denaturation of the tryptophan synthase alpha subunit. Evidence that the equilibrium intermediate is a molten globule. *J. Mol. Biol. 234*, 1197−1206.
4. Jeng, M.f., and Englander, S. W., (1991) Stable submolecular folding units in a non- compact form of cytochrome *c*. *J. Mol. Biol. 221*, 1045−1061.
5. Goto, Y., Takahashi, N., and Fink, A. L. (1990) Mechanism of a acid-induced folding of proteins. *Biochemistry 29*, 3480−3488.
6. Chalikian, T. V., Gindikin, V. S., and Breslauer, K. J. (1996) Spectroscopic and volumetric investigation of cytochrome *c* unfolding at alkaline pH: characterization of the base-induced unfolded state at 25 °C. *FASEB 10*, 164−170.
7. Kuroda, Y., Kidokoro, S−i., and Wada, A. (1992) Thermodynamic characterization of cytochrome *c* at low pH. Observation of molten globule state and of cold denaturation process. *J. Mol. Biol. 223*, 1139−1153.
8. Ali, V., Prakash, K., Kulkarni, S., Ahmad, A., Madhusudan, K. P., and Bhakuni, V. (1999) 8-Anilino-1-naphthalene sulfonic acid (ANS) induces folding of cytochrome *c* to molten globule state as a result of electrostatic interactions. *Biochemistry 38*, 13635−13642.
9. Hagihara, Y., Tan, Y., and Goto, Y. (1994) Comparison of the conformational stability of the molten globule and native states of cytochrome *c*: effects of acetylation, urea and guanidine-hydrochloride. *J. Mol. Biol. 237*, 336−348.
10. Myer, Y. P., MacDonald, L. H., Verma, B. C., and Pande, A. (1980) Urea denaturation of horse heart cytochrome *c*. Equilibrium studies and characterization of intermediate forms. *Biochemistry 19*, 199−207.
11. Ferri, T., Poscia, A., Ascoli., F., and Santucci., R. (1996) Direct electrochemical evidence for an equilibrium intermediate in the guanidine-induced unfolding of cytochrome *c*. *Biochim. Biophys. Acta 1298*, 102−108.
12. Thomas, Y. G., Goldbeck, R. A., and Kliger, D. S. (2000) Characterization of equilibrium intermediates in denaturant induced unfolding of ferrous and ferric cytochromes c using magnetic circular dichroism, circular dichroism, optical absorption spectroscopies. *Biopolymers 57*, 29−36.
13. Ahmad, F., and Bigelow, C. C. (1979) The denaturation of ribonuclease A by combination of urea and salt denaturant. *J. Mol. Biol. 131*, 607−617.
14. Ahmad, F. (1983) Free energy changes in ribonuclease A: effect of urea, guanidine hydrochloride and lithium salts. *J. Biol. Chem. 258*, 11143−11146.
15. Ahmad, F. (1984) Free energy changes in denaturation of ribonuclease A by mixed denaturants. *J. Biol. Chem. 259*, 4183−4186.
16. Ahmad, F. (1985) Thermodynamic characterization of the partially denatured states of ribonuclease A in calcium chloride and lithium chloride. *Can. J. Biochem. Cell Biol. 63*, 1058−1063.
17. Ahmad, Z., and Ahmad, F. (1992) Mechanism of denaturation of cytochrome *c* by lithium salts. *Ind. J. Chem. 31B*. 874−879.
18. Ahmad, Z., and Ahmad, F. (1994) Physicochemical characterization of products of unfolding of cytochrome *c* by calcium chloride. *Biochim. Biophys. Acta 1207*, 223−230.
19. Ahmad, Z., Yadav, S., Ahmad, F., and Khan, N. Z. (1996) Effects of salts of alkali earth metals and calcium chloride on the stability of cytochrome-c and myoglobin. *Biochim. Biophys. Acta 1294*, 63−71.
20. Margoliash, E., and Forhwirt, N. (1959) Spectrum of horse heart cytochrome *c*. *Biochem. J. 71*, 570−572.
21. Weast, R. C. (1972) *CRC Handbook of Chemistry and Physics*, 53rd ed.; CRC Press, Cleveland, OH.
22. Mulqueen, P. M., and Kronman, M. J. (1982) Binding of naphthalene dyes to the N and A conformers of bovine alpha-lactalbumin. *Arch. Biochem. Biophys. 215*, 28−39.
23. Ahmad, F., and Salahuddin, A. (1976) Reversible unfolding of the major fraction of ovalbumin by guanidine hydrochloride. *Biochemistry 15*, 5168−5174.
24. Stellwagen, E. (1968) The reversible unfolding of horse heart cytochrome *c*. *Biochemistry 7*, 2893−2898.
25. Ahmad, F., and Bigelow, C. C. (1982) Estimation of free energy of stabilization of ribonuclease-A, lysozyme, alpha-lactalbumin and myoglobin. *J. Mol. Biol. 257*, 12935−12940.
26. Drew, H. R., and Dickerson, R. E. (1978) Unfolding of the cytochrome *c* in methnol and acid. *J. Biol. Chem 253*, 8420−8427.
27. Ikai, A., Fish., W. W., and Tanford, C. (1973) Kinetics of unfolding and refolding of protein. II Results of cytochrome *c*. *J. Mol. Biol. 73*, 165−184.
28. Pace, C. N. (1975) The stability of globular proteins CRC *Crit. Rev. Biochem. 3*, 1−43.
29. Czernuszewicz, R. S., Li, C.-Y., and Spiro, T. G. (1989) Nickel octaethylporyphyrin ruffling dynamics from resonance Raman spectroscopy. *J. Am. Chem. Soc. 111*, 7024−7031.
30. Yang, J. T., Wu, C. C., and Martinez, H. M. (1986) Calculation of protein conformation from circular dichroism. *Methods Enzymol. 130*, 208−269.
31. Davies, A. M., Guillemette, J. G., Smith, M., Greenwood, C., Thurgood, A. G. P., Mauk, A. G., and Moore, G. R. (1993) Redesign of the interior hydrophilic region of mitochondrial cytochrome *c* by site-directed mutagenesis. *Biochemistry 32*, 5431−5435.
32. Tanford, C. (1961) "Physical Chemistry of Macromolecule," Wiley, New York.
33. Taneja, S., and Ahmad, F. (1994) Increased thermal stability of proteins in the presence of amino acids. *Biochem. J. 303*, 147−153.
34. Knapp, J. A., and Pace, C. N. (1974) Guanidine hydrichloride and acid denaturation of horse, cow and *candida krusei* cytochromes c. *Biochemistry 13*, 1289−1294.
35. Semisotnov, G. V., Rodionova, N. A., Razgulayev, O. I., Uversky, V. N., Grapias, A. F., and Gilmanshin, R. I. (1991) Study of the "molten globule" intermediate state in protein folding by a hydrophobic fluorescent probe. *Biopolymers 31*, 119−128.
36. Ptitsyn, O. B. (1995) Molten globule and protein folding. *Adv. Protein Chem. 47*, 83−229.
37. Hamada, D., Kuroda, Y., Katoka, M., Aimoto, S., Yoshimura, T., and Goto., Y. (1996) Role of axial ligands in the conformational stability of the native and molten globule state of cytochrome *c*. *J. Mol. Biol. 256*, 172−186.
38. Ohgushi, M. and Wada, A. (1983) 'Molten-globule state': a compact form of globular proteins with mobile side-chains. *FEBS Lett. 164*, 21−24.
39. Akiyama, S., Takahashi, S., Kimura, T., Ishimori, K., Morishima, I., Nishikawa, Y. and Fujisawa, T. (2002) Conformational landscape of cytochrome *c* folding studied by microsecond-resolved small-angle X-ray scattering. *Proc. Natl. Acad. Sci. U.S.A. 99*, 1329−1334.
40. Freire, E. (1995) Thermodynamics of partly folded intermediates in proteins. *Annu. Rev. Biophys. Biomol. Struct. 24*, 141−165.
41. Pfeil, W. (1998) *Protein Stability and Folding. A Collection of Thermodynamic Data*; Springer-Verlag, Heidelberg, New York; pp 383−389.
42. Vassilenko, K. S., and Uversky, V. N. (2002) Nativelike secondary structure of molten globules. *Biochim. Biophys. Acta 1594*, 168−177.
43. Davis-Searles, P. R., Morar, A. S., Saunders, A. J., Erie, D. A., and Pielak, G. J. (1998) Sugar-induced molten globule model. *Biochemistry 37*, 17048−17053.

44. Makhatadze, G. I., Clore, G. M., Groneborn, A. M. (1995) Solvent isotope effect and protein stability. *Nat. Struct. Biol. 2*, 852−855.
45. Barrick, D., and Baldwin, R. L. (1993) The molten globule intermediate of apomyoglobin and the process of protein folding. *Protein Sci. 2*, 869−876.
46. Dickerson, R. E., Takano, T., Eisenberg, D., Kallia, O. B., Samson, L., Cooper, A., and Margoalish, E. (1971) Ferricytochrome *c* 1. General features of horse and bonito proteins at 2.8 Å resolution. *J. Biol. Chem. 246*, 1511−1535.
47. Fisher, W. R., Taniuchi, H., and Anfinsen, C. B. (1973) The role of heme in the formation of the structure of cytochrome *c*. *J. Biol. Chem. 248*, 3188−3195.
48. Griko, Y. V., Freire, E., and Privalov, P. L. (1994) Energetics of the alpha-lactalbumin states. A calorimetric and statistical thermodynamic study. *Biochemistry 33*, 1889−1899.
49. Carra, J. H., Elizabeth, A. A., and Privalov, P. L. (1994) Thermodynamics of staphylococcal nuclease denaturation. I. The acid denatured state. *Protein Sci. 3*, 944−951.
50. Potekhin, S., and Pfeil, W. (1989) Microcalorimetric studies of conformational transitions of ferricytochrome *c* in acidic solutions. *Biophys. Chem. 34*, 55−62.
51. Bychkova. V. E., Dujsekina, A. E., Klenin, S. I., Tiktopulo, E. I., Uversky, V. N., and Ptitsyn, O. B. (1996) Molten globule like state of cytochrome *c* under conditions stimulating those near the membrane surface. *Biochemistry 35*, 6058−6063.
52. Schartz, G. (1993) The protein import machinery of mitochondria. *Protein Sci. 2*, 141−146.

BI0271042